

1998

# Characterization of Gas Atomized Cu<sub>48</sub>Ti<sub>34</sub>Zr<sub>10</sub>Ni<sub>8</sub> Amorphous Alloy

J. C. Foley

*Iowa State University*

D. J. Sordelet

*Iowa State University*

Thomas A. Lograsso

*Iowa State University*, [lograsso@ameslab.gov](mailto:lograsso@ameslab.gov)

Follow this and additional works at: [http://lib.dr.iastate.edu/ameslab\\_conf](http://lib.dr.iastate.edu/ameslab_conf)



Part of the [Metallurgy Commons](#)

## Recommended Citation

Foley, J. C.; Sordelet, D. J.; and Lograsso, Thomas A., "Characterization of Gas Atomized Cu<sub>48</sub>Ti<sub>34</sub>Zr<sub>10</sub>Ni<sub>8</sub> Amorphous Alloy" (1998). *Ames Laboratory Conference Papers, Posters, and Presentations*. 39.  
[http://lib.dr.iastate.edu/ameslab\\_conf/39](http://lib.dr.iastate.edu/ameslab_conf/39)

This Conference Proceeding is brought to you for free and open access by the Ames Laboratory at Iowa State University Digital Repository. It has been accepted for inclusion in Ames Laboratory Conference Papers, Posters, and Presentations by an authorized administrator of Iowa State University Digital Repository. For more information, please contact [digirep@iastate.edu](mailto:digirep@iastate.edu).

---

# Characterization of Gas Atomized Cu<sub>48</sub>Ti<sub>34</sub>Zr<sub>10</sub>Ni<sub>8</sub> Amorphous Alloy

## Abstract

The advent of multi-component metallic alloys, which exhibit relatively good glass forming ability, has opened opportunities for processing metallic glasses into thick cross section components. The relatively good glass forming ability is important because conventional processing techniques (e.g., casting, extrusion and rolling) may be used to fabricate useful shapes while retaining the excellent engineering properties of an amorphous structure. In particular, the favorable processing characteristics of bulk amorphous alloys are the low cooling rates which can be exercised to yield an amorphous structure and the operating temperature range between the glass transition temperature ( $T_g$ ) and the crystallization temperature ( $T_x$ ). Current work is focused on developing a processing strategy that will allow us to fabricate even larger cross section amorphous alloys than are currently achievable by casting methods. The technique involves producing high pressure gas atomized (HPGA) Cu<sub>48</sub>Ti<sub>34</sub>Zr<sub>10</sub>Ni<sub>8</sub> powders and consolidating them at temperatures above  $T_g$ , but below  $T_x$ . Thermal analysis of atomized powders by DSC provides details of the influence of powder particle size, which is related to cooling rate during atomization. The results of experiments characterizing the thermal and kinetic behavior of Cu<sub>48</sub>Ti<sub>34</sub>Zr<sub>10</sub>Ni<sub>8</sub> powders indicate that short processing times are required to retain the amorphous structure during consolidation in the temperature regime between  $T_g$  and  $T_x$ .

## Disciplines

Metallurgy

## Comments

This article is from *MRS Proceedings* 554 (1998): 199, doi:[10.1557/PROC-554-199](https://doi.org/10.1557/PROC-554-199).

# CHARACTERIZATION OF GAS ATOMIZED $\text{Cu}_{48}\text{Ti}_{34}\text{Zr}_{10}\text{Ni}_8$ AMORPHOUS ALLOY

J. C. FOLEY, D. SORDELET, AND T. A. LOGRASSO

Ames Laboratory, Iowa State University, Ames, IA 50011

## ABSTRACT

The advent of multi-component metallic alloys, which exhibit relatively good glass forming ability, has opened opportunities for processing metallic glasses into thick cross section components. The relatively good glass forming ability is important because conventional processing techniques (e.g., casting, extrusion and rolling) may be used to fabricate useful shapes while retaining the excellent engineering properties of an amorphous structure. In particular, the favorable processing characteristics of bulk amorphous alloys are the low cooling rates which can be exercised to yield an amorphous structure and the operating temperature window between the glass transition temperature ( $T_g$ ) and the crystallization temperature ( $T_x$ ). Current work is focused on developing a processing strategy that will allow us to fabricate even larger cross section amorphous alloys than are currently achievable by casting methods. The technique involves producing high pressure gas atomized (HPGA)  $\text{Cu}_{48}\text{Ti}_{34}\text{Zr}_{10}\text{Ni}_8$  powders and consolidating them by warm hydrostatic extrusion at temperatures above  $T_g$ , but below  $T_x$ . Thermal analysis of atomized powders by DSC provides details of the influence of powder particle size, which is related to cooling rate during atomization. The results of experiments characterizing the thermal and kinetic behavior of  $\text{Cu}_{48}\text{Ti}_{34}\text{Zr}_{10}\text{Ni}_8$  powders indicate that short processing times are required to retain the amorphous structure during consolidation.

## INTRODUCTION

The first report of metallic glass formation during continuous cooling from the melt [1] sparked numerous experiments dealing with non-crystalline metallic solids. Many of these reports have involved systems that are capable of producing amorphous materials by various rapid solidification techniques that achieve very large cooling rates ( $10^5$ - $10^8$  K/s) such as splat-quenching or melt-spinning. It wasn't until 1974 that the first reported bulk metallic glasses, cylindrical rods 1 to 3 mm in diameter of Pd-Cu-Si, Pd-Ni-P and Pt-Ni-P, were reported by Chen [2]. More recently, Inoue and coworkers [3, 4] have reported the formation of amorphous multicomponent alloys that do not contain relatively expensive Pd and Pt. In addition to greater glass formability, these bulk amorphous alloys also exhibited desirable mechanical properties and a reported wide supercooled liquid range. The presence of a wide supercooled liquid range gave rise to the promise of novel near-net shape deformation processes to form relatively large structural components of metallic glasses [5]. Recently, a successful synthesis of glassy alloy compacts with full strength by warm extrusion of atomized glassy powder in the supercooled liquid state was reported [6].

In principle, powder metallurgy (P/M) processing of amorphous powder could be applied to any amorphous alloy that can be atomized and exhibits a wide supercooled region. The ability to fabricate rod and sheet stock of high strength, high fracture toughness amorphous alloys will open the possibility for many technical applications. However, before successful consolidation of amorphous metals becomes common place, a clear understanding of the formation and stability of powder amorphous alloys is needed. In general, crystallization of amorphous alloys occurs by nucleation and growth processes [7], but several decomposition pathways have been reported [7-10]. A determination of the decomposition pathways active in  $\text{Cu}_{48}\text{Ti}_{34}\text{Zr}_{10}\text{Ni}_8$  is required to set consolidation processing parameters.

A bulk amorphous sample with the composition  $\text{Cu}_{47}\text{Ti}_{34}\text{Zr}_{10}\text{Ni}_8$  is reported to exhibit a  $T_g$  at  $398^\circ\text{C}$ ,  $T_x$  at  $444^\circ\text{C}$  and  $\Delta T = 46^\circ\text{C}$  [11]. In addition, the critical cooling rate is reported to be less than  $250^\circ\text{C/s}$ . While the wide supercooled region and relatively low critical cooling rate should enable production of amorphous powder, it is unclear how the increased surface area and change in cooling rate as a function of powder size will affect the decomposition pathways.

## EXPERIMENT

An ingot of the composition  $\text{Cu}_{48}\text{Ti}_{34}\text{Zr}_{10}\text{Ni}_8$  was made by induction melting 99.99% pure Ti, 99.99% pure Zr, 99.999% pure Cu, and 99.99% pure Ni in a graphite crucible. The ingot material was high pressure gas atomized (HPGA) at Ames Laboratory using a hard fired  $\text{Al}_2\text{O}_3$  bottom pour crucible and 99.99% pure argon gas. A portion of the powder obtained from HPGA was classified into the size categories of diameter  $< 5 \mu\text{m}$ , diameter  $5 \mu\text{m}$ - $15 \mu\text{m}$ , diameter  $15 \mu\text{m}$ - $25 \mu\text{m}$ ,  $25 \mu\text{m}$ - $38 \mu\text{m}$ ,  $38 \mu\text{m}$ - $45 \mu\text{m}$ ,  $45 \mu\text{m}$ - $53 \mu\text{m}$ ,  $53 \mu\text{m}$ - $62 \mu\text{m}$ ,  $62 \mu\text{m}$ - $75 \mu\text{m}$ ,  $75 \mu\text{m}$ - $90 \mu\text{m}$ , and  $90 \mu\text{m}$ - $106 \mu\text{m}$ . Select samples of the classified powder were examined by a Perkin-Elmer Pyris1 differential scanning calorimeter (DSC), x-ray diffraction (XRD) using a Cu K  $\alpha$  source, and scanning electron microscopy (SEM). The starting ingot and HPGA powder in the range of diameter  $75$ - $106 \mu\text{m}$  and diameter  $< 75 \mu\text{m}$  was examined with inductively coupled plasma (ICP) and inert gas fusion (IGF) techniques. In addition, a small arc-cast ingot was made for comparison to the HPGA powder.

## RESULTS

Chemical analysis of the starting ingot indicated that the carbon content was well below 100 ppmw and that the alloy composition was similar to the desired nominal composition.

Chemical analysis results of the powder in the range of diameter 75-106  $\mu\text{m}$  and diameter < 75  $\mu\text{m}$  are shown in Table 1. Although the chemical analysis results indicate that the copper content is slightly higher than the nominal composition and the titanium content is slightly lower than nominal, the compositions of the two powder samples are very similar.

Table 1  
Chemical composition results of the HPGA powder

Sample	Cu (at%)	Ti (at%)	ZR (At%)	Ni (at%)	O (ppmw)	N (ppmw)
75-106 $\mu\text{m}$	52.4	30	9.5	8.1	762	<1
< 75 $\mu\text{m}$	54.6	29.4	9.3	6.7	855	1

The X-ray diffraction trace of a slice of the arc-cast ingot is shown in Figure 1. From the x-ray diffraction trace shows strong evidence of crystalline peaks with some evidence of amorphous scattering. In contrast, the x-ray diffraction traces of the HPGA powder shown in Figure 2 only exhibit amorphous scattering maximums. The location of the amorphous scattering maximums occurs at the same two-theta values. The presence of the amorphous scattering maximums in the same locations is an indication that all of the powder no matter what the diameter is amorphous.

The continuous DSC traces of select  $\text{Cu}_{48}\text{Ti}_{34}\text{Zr}_{10}\text{Ni}_8$  HPGA powder sizes at  $40^\circ\text{C}/\text{min}$  are shown in Figure 3. The traces were normalized to the sample weights and overlaid for comparison. All of the continuous DSC traces exhibit a glass transition ( $T_g$ ) signal around  $440^\circ\text{C}$  and crystallization temperature ( $T_x$ ) around  $480^\circ\text{C}$ . In addition, all of the subsequent reactions are the same and occur at the same temperatures. The presence of the  $T_g$  signal around  $440^\circ\text{C}$  is strong evidence that all the powder sizes evaluated are completely amorphous. The

isothermal DSC traces of the  $< 5 \mu\text{m}$  and  $90\text{-}106 \mu\text{m}$  powder are shown in Figure 4. Again, the thermal signal from the very small powder is very similar to the signal of the very large powder. The differences in onset time, peak time and  $\Delta H$  associated with the decomposition reaction are negligible.

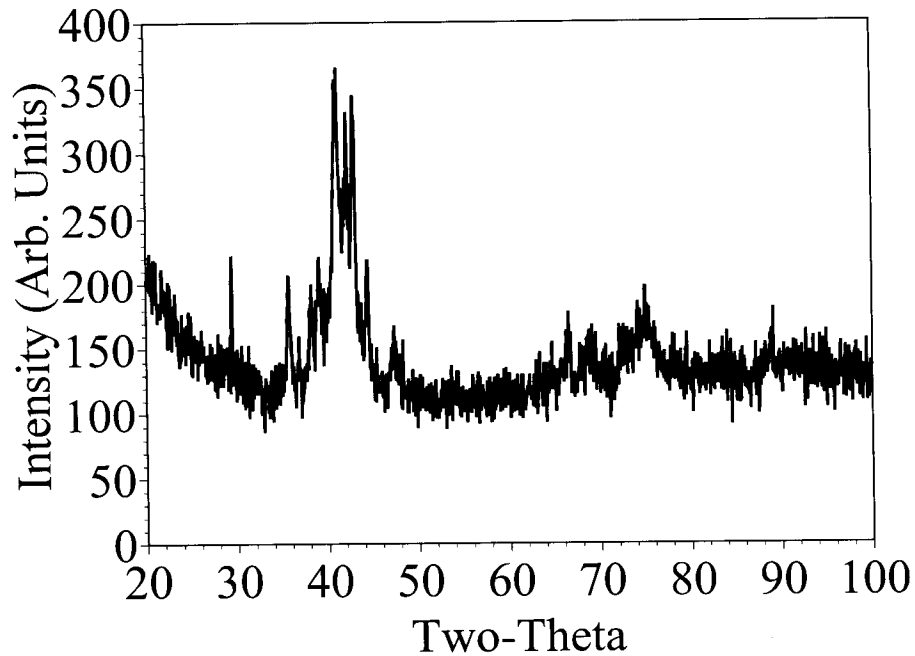


Figure 1. The X-ray diffraction trace of the arc-cast  $\text{Cu}_{48}\text{Ti}_{34}\text{Zr}_{10}\text{Ni}_8$  alloy.

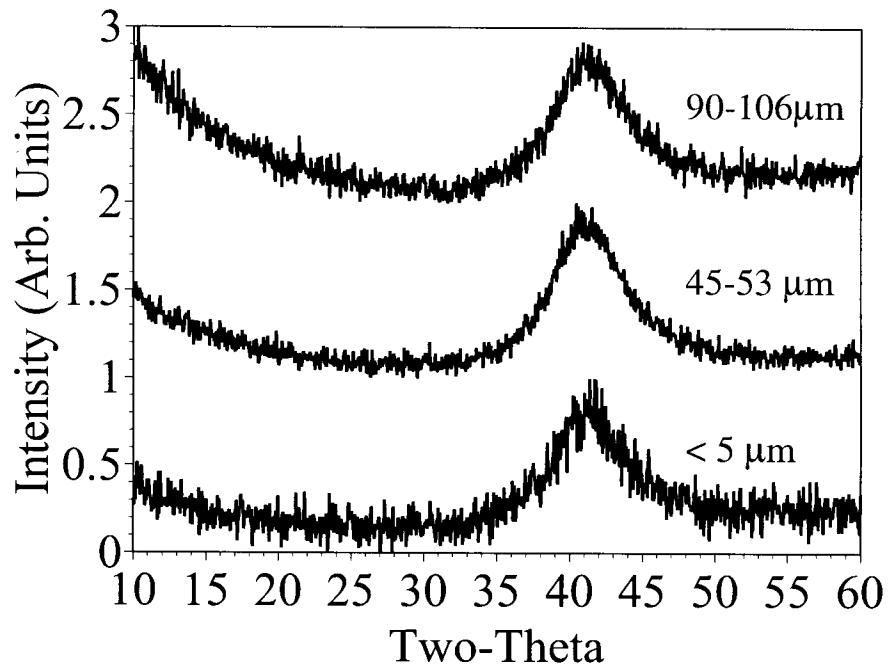


Figure 2. The X-ray diffraction traces of the  $\text{Cu}_{48}\text{Ti}_{34}\text{Zr}_{10}\text{Ni}_8$  HPGA powder.

New samples of  $< 5 \mu\text{m}$  and  $90\text{-}106 \mu\text{m}$  powder were annealed at  $450^\circ\text{C}$  for 3 minutes to partially crystallize the powder. Samples of the partially crystallized powder were examined with SEM and are shown in Figures 5A and 5B. The SEM micrographs show no evidence of crystalline phase. The continuous DSC traces of the  $< 5 \mu\text{m}$  powder conducted at  $5^\circ\text{C}/\text{min}$  and  $40^\circ\text{C}/\text{min}$  are shown in Figure 6. From the traces shown in Figure 6, it is apparent that the thermal signal obtained at the different heating rates are quite different.



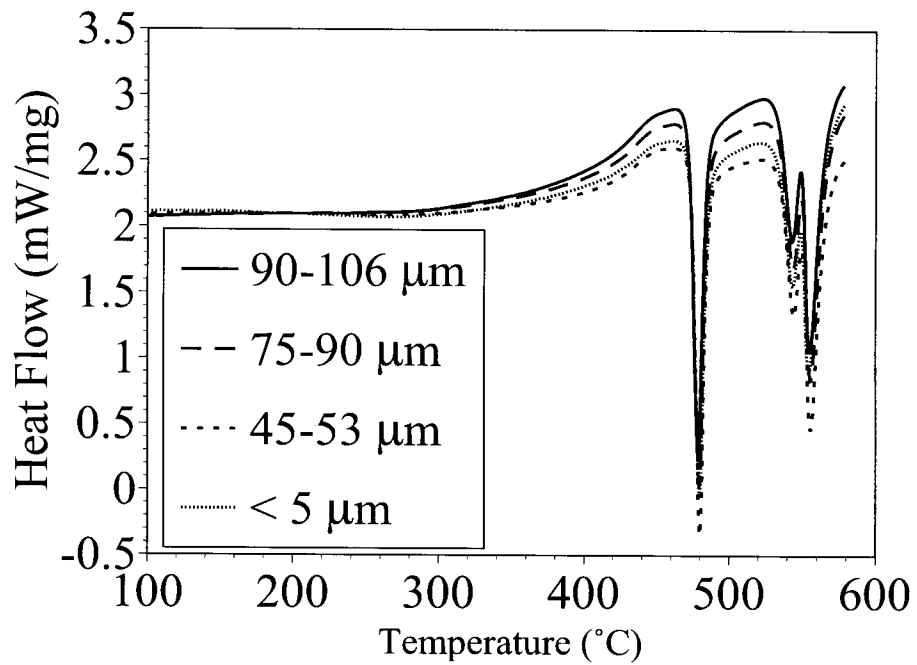


Figure 3. The continuous DSC traces of select  $\text{Cu}_{48}\text{Ti}_{34}\text{Zr}_{10}\text{Ni}_8$  HPGA powder sizes at  $40^\circ\text{C}/\text{min}$ .

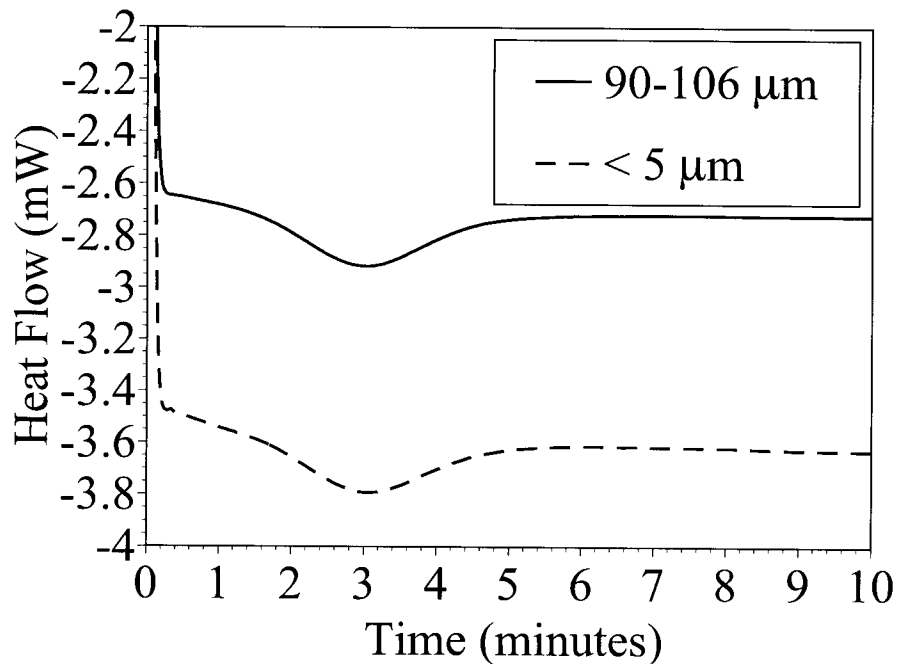


Figure 4. The isothermal DSC traces of the  $< 5 \mu\text{m}$   $90\text{-}106 \mu\text{m}$   $\text{Cu}_{48}\text{Ti}_{34}\text{Zr}_{10}\text{Ni}_8$  HPGA powder at  $450^\circ\text{C}$ .

## Pretty Pictures

Figure 5. The SEM micrographs of the  $< 5 \mu\text{m}$  and  $90\text{-}106 \mu\text{m}$  after annealing at  $450^\circ\text{C}$  for 3 minutes.

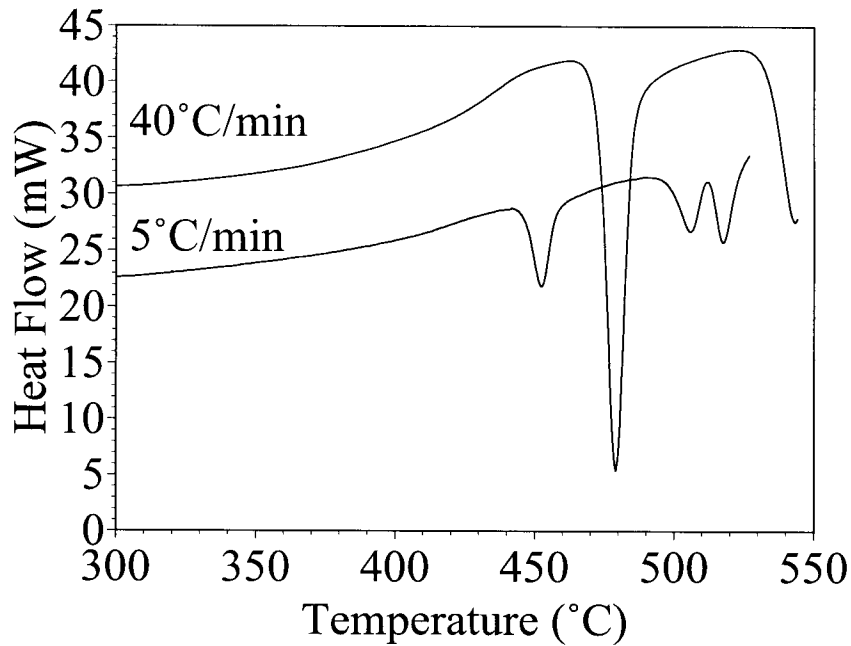


Figure 6. The continuous DSC traces of the  $< 5 \mu\text{m}$   $\text{Cu}_{48}\text{Ti}_{34}\text{Zr}_{10}\text{Ni}_8$  HPGA powder at  $5^\circ\text{C}/\text{min}$  and  $40^\circ\text{C}/\text{min}$ .

## DISCUSSION

The  $\text{Cu}_{48}\text{Ti}_{34}\text{Zr}_{10}\text{Ni}_8$  powders made by HPGA appear to be completely amorphous and exhibit the same  $T_g$ ,  $T_x$ , and decomposition kinetics. It appears that the same nucleation site is active in both the large ( $90\text{-}106 \mu\text{m}$ ) and small ( $< 5 \mu\text{m}$ ) powder sizes. This is an indication that the powder surface of these powders is not a strong nucleation site for the crystallization of the amorphous powder. If the powder surface were a strong nucleation site, it would stand to reason that the smaller powder particles would have a much higher density of potent sites, which should cause a noticeable difference in the decomposition behavior. In contrast, if the powder contained a high density ( $> 10^{20} \text{m}^{-3}$ ) of internal sites, as other amorphous forming alloys seem to contain

[12], the different powder sizes examined in this work would exhibit similar decomposition behavior.

While it is likely that internal heterogeneous nucleation is the rationale for the observance of similar thermal decomposition signals, it is unclear what type of heterogeneous nucleant is active in the  $\text{Cu}_{48}\text{Ti}_{34}\text{Zr}_{10}\text{Ni}_8$  HPGA powder. As mentioned previously, other amorphous forming alloys are reported to contain a high density of heterogeneous nucleants that can be bypassed with relatively high continuous cooling rates [12]. Another possible source of nucleants is a result of phase separation that has been reported to occur in some bulk amorphous alloys [8]. The current study can not resolve this issue, but if phase separation is occurring two  $T_g$  reactions should exist for each of the two amorphous phases [7]. Moreover, examination of the partially crystallized powders with transmission electron microscopy could elucidate the most likely decomposition route.

## CONCLUSIONS

The formation of amorphous  $\text{Cu}_{48}\text{Ti}_{34}\text{Zr}_{10}\text{Ni}_8$  powder was successfully made by HPGA. All of the powder diameters evaluated were completely amorphous and exhibited the same decomposition pathway and kinetics. It is likely that the same nucleation sites are active in both the  $< 5 \mu\text{m}$  and  $90\text{-}106 \mu\text{m}$  powder. A wide supercooled region was only observed when the powder was heated at  $40^\circ\text{C}/\text{min}$ . Slower heating rates resulted in different decomposition reactions to occur. The relatively short crystallization delay time of the  $\text{Cu}_{48}\text{Ti}_{34}\text{Zr}_{10}\text{Ni}_8$  powder at  $450^\circ\text{C}$  will make consolidation of the powder into a completely amorphous compact difficult. Further investigations of the decomposition pathway and kinetics are needed.

## ACKNOWLEDGEMENTS

The authors would like to acknowledge the financial support of the Materials Science Division of DOE/BES under contract number W-7405-Eng-82 and a Special Research Initiation Grant from the Office of the Vice Provost, Iowa State University. Thanks also go to Amy Ross for her help in obtaining SEM micrographs, to John Wheelock for his help in the fabrication of arc-cast rods and to Chris Gross for the chemical analysis.

## REFERENCES

1. P. Duwez, R.H. Willens, and W. Klement, *Appl. Phys. Lett.*, **31**, 1136-1150, (1960).
2. H.S. Chen, *Acta Met.*, **22**, 1505, (1974).
3. A. Inoue, T. Zhang, and T. Masumoto, *Mater. Trans. JIM*, **31**, 177-183, (1990).
4. T. Zhang, A. Inoue, and T. Masumoto, *Mater. Trans. JIM*, **32**, 1005-1010, (1991).
5. T. Masumoto, *Sci. Rep. RITU*, **A39**, 98-101, (1994).
6. Y. Kawamura, H. Kato, A. Inoue, and T. Masumoto, *International Journal of Powder Metallurgy*, **33**, 50-61, (1997).
7. U. Köster and U. Herold, *Topics in Applied Physics*, **46**, 225-259, (1981).
8. S. Schneider, P. Thiyagarajan, and W.L. Johnson, *Appl. Phys. Lett.*, **68**, 493-495, (1996).
9. J.C. Foley, D.R. Allen, and J.H. Perepezko, *Scripta Materialia*, **35**, 655-660, (1996).
10. D.R. Allen, J.C. Foley, and J.H. Perepezko, *Acta Mater.*, **46**, 431-440, (1998).
11. X.H. Lin and W.L. Johnson, *J. Appl. Phys.*, **78**, 6514-6519, (1995).
12. J.C. Foley, H. Sieber, D.R. Allen, and J.H. Perepezko. "The Effect of Processing on the Microstructural Evolution During Solidification of Al-Y-Fe Glass Forming Alloys". *The 4th Decennial International Conference on Solidification Processing* 1997. p. 602-605.